

Toward Homogenization of Heterogeneous Metal Nanoparticle Catalysts with Enhanced Catalytic Performance: Soluble Porous Organic Cage as a Stabilizer and Homogenizer

Jian-Ke Sun, Wen-Wen Zhan, Tomoki Akita, and Qiang Xu*

National Institute of Advanced Industrial Science and Technology (AIST), Ikeda, Osaka 563-8577, Japan

S Supporting Information

ABSTRACT: Organic molecular cage (CC3-R) with intrinsically porous skeleton is used as a support for immobilizing Rh nanoparticles (NPs) in an ultrasmall size of ~ 1.1 nm for the first time. The CC3-R with the unique characteristic of high solubility can be utilized to homogenize the heterogeneous catalyst in solution. The obtained homogenized heterogeneous catalyst Rh/CC3-R-*homo* exhibits significantly enhanced catalytic performance toward various liquid-phase catalytic reactions, as compared with the heterogeneous counterpart Rh/CC3-R-*hetero*. Moreover, Rh/CC3-R-*homo* shows excellent durability and recyclability. The advantage of combining homogeneous and heterogeneous catalysts is likely to be beneficial for many applications.

The newly emerging open frameworks, such as metal–organic frameworks (MOFs) and porous organic frameworks (POFs), have been targeted as particularly attractive supports for heterogeneous metal nanoparticle (MNP) catalysts over the past several years.¹ The highly tunable pore structures and high porosities of these kinds of materials open a new avenue for the synthesis of heterogeneous catalysts with high catalytic performance in various catalytic reactions.² Generally, control of MNP size, shape, and dispersity is the key to enhance the activity of these kinds of catalysts.³ Despite the great progresses that have been achieved over the past few years, it is still a great challenge to deliberately control these factors and optimize the synthesis condition for the performance of the catalysts. For example, the contradiction of decreased size of MNPs will lead to high surface energy, which is prone to agglomerate or change shape during catalytic reactions, especially, for the weak interaction between the porous support and MNPs, resulting in a dramatic decrease of their activity. Therefore, the development of facile and general method to improve the catalytic performance of porous support-immobilized MNP catalysts is highly desirable.

It is well-known that the homogeneous catalysts are generally more active than their heterogeneous counterparts because of the well-dispersed catalytic sites in solution, which are highly accessible and favorable for the kinetic performance of the catalysis.⁴ As for heterogeneous catalysts such as porous support-immobilized MNPs, the effective contact between the MNPs and reactants often suffers from the diffusion problem, which leads to a slow kinetic performance of catalysts.⁵ Although the surfactant-protected MNPs have a good dispersibility in solution, the long alkyl chains grafted on the MNPs generally block the direct

contact between the MNPs and reactants, resulting in a negative effect on the catalytic activity.⁶ One of the major goals in catalysis is to combine the advantages of molecular catalysts and heterogeneous processes, ideally maintaining or even improving the activity of the resultant catalysts, while facilitating the recovery and recycling.⁷ However, catalysts that allow selective control of both modes are extremely rare.⁸

Herein, for the first time, we demonstrate a facile method of enhancement of liquid-phase catalytic performance by homogenizing the heterogeneous catalysis on the basis of a porous support-immobilized MNP catalyst. As a proof of concept, we employ a porous organic molecule, CC3-R,⁹ a class of [4 + 6] cycloimine cage with an intrinsically porous structure, as a novel support for immobilizing MNPs. The main feature of CC3-R is its good solubility in certain solvents with well-kept prefabricated open skeleton,^{9b} which provides an ideal platform for homogenizing the catalysis in solution. To demonstrate the feasibility of this method, the CC3-R-supported Rh NPs are prepared in a solution process and used as catalysts for catalytic reactions. The resultant homogenized heterogeneous catalyst Rh/CC3-R-*homo* gives a solution without any precipitation, which resembles a homogeneous catalytic system upon mixing with reactants. Such “soluble” nanocatalyst has several remarkable features including (1) high stability and dispersibility in solution, (2) effective control of MNPs in an ultrasmall size of ~ 1.1 nm, (3) significant enhancement of catalytic activity toward liquid-phase reactions as compared with the heterogeneous counterpart as in a form of solid, and (4) excellent durability and reusability, which are likely to be beneficial for many applications.

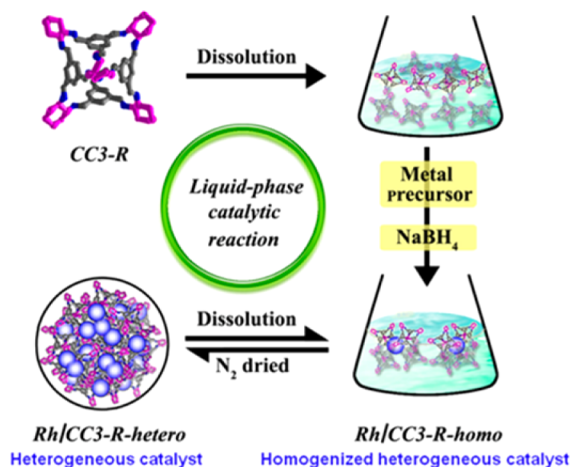
The CC3-R is synthesized according to a previous literature.⁹ The channel diameter in CC3-R varies between 0.58 nm at the narrowest point within the triangular cage window to 0.72 nm within the cage itself. The phase purity of solid CC3-R is verified by powder X-ray diffraction (PXRD) measurements, which is consistent with a calculation from the single crystal data (Figure S1). The N₂ sorption measurement shows that the specific surface area of CC3-R is 452 m² g⁻¹, demonstrating the intrinsically porous characteristic (Figure S2). The solid CC3-R is insoluble in strong polar solvents like alcohol and water but can completely dissolve in dichloromethane or a dichloromethane–alcohol mixture under certain volume ratio with maintaining the prefabricated skeleton.

Received: April 19, 2015

Published: May 28, 2015

The Rh/CC3-R-*homo* catalyst could be easily prepared by a solution process (Scheme 1). Briefly, a solution (12 mL) of

Scheme 1. Schematic Illustration of Preparation of Homogenized Heterogeneous Catalyst and Its Heterogeneous Counterpart



dichloromethane and methanol mixture (volume ratio = 2:1) was added to a flask containing dried CC3-R (80 mg) to give a colorless solution (Figure S3). The color of solution became yellow upon adding the rhodium acetate. After aging for 20 min, the mixture was subsequently reduced with a methanol solution of sodium borohydride (9 mg, rt). The solution immediately changed color from yellow to dark brown without any precipitates, indicating efficient Rh(II) reduction and further stabilization of the resulting Rh NPs by CC3-R. The conversion of Rh(II) to Rh(0) can be followed in the UV–vis absorption spectra taken during the reaction (Figure S4). The disappearance of adsorption band of Rh(II) at 361 nm upon addition of NaBH₄ into the solution indicates that the metal ions are reduced completely in the present system.¹⁰

The Rh NP diameter and size distribution were analyzed using transmission electron microscopy (TEM). The sample was prepared using a solution of Rh/CC3-R-*homo* catalyst with 10-fold dilution. The solution was drop-cast onto carbon-coated copper grids and allowed to dry before the measurements. The TEM image of Rh/CC3-R-*homo* shows the formation of well-dispersed Rh NPs (Figure 1a). The morphology of Rh NPs was further revealed by high-angle annular dark-field scanning transmission electron microscopy (HAADF-STEM) images (Figure 1b,c). The average diameter of Rh NPs is 1.1 ± 0.2 nm, and about ~9% of Rh NPs have particle sizes smaller than the estimated cage internal cavity size (0.72 nm), indicating that most of the particles are anchored on the surface of CC3-R. Energy-dispersive X-ray spectroscopy (EDS) elemental mapping of Rh/CC3-R-*homo* shows the well-dispersed Rh NPs stabilized by CC3-R (Figure S5). X-ray photoelectron spectroscopy (XPS) analysis also identifies the formation of Rh NPs with binding energies at 307.5 and 312.2 eV (Figure S6), corresponding to Rh 3d_{5/2} and Rh 3d_{3/2} of metallic Rh, respectively.

Despite the ultrasmall size, Rh/CC3-R-*homo* catalyst shows excellent stability. It is stable in solution, with no evidence of agglomeration, and without noticeable color change, over periods of days. More importantly, it can be dried under N₂ flow atmosphere and then redissolved in a solution of dichloromethane–methanol mixture (volume ratio = 2:1) with

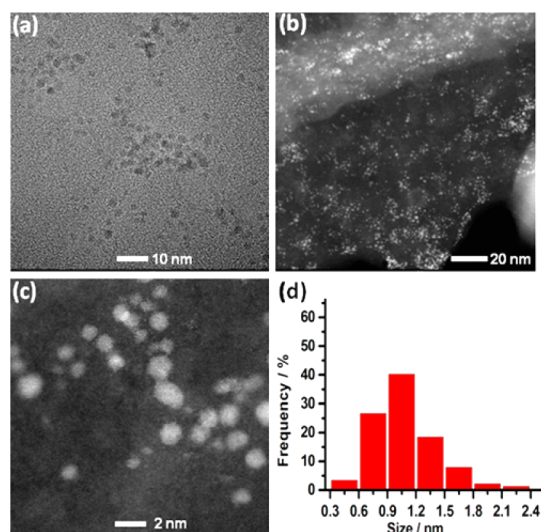


Figure 1. (a) TEM and (b,c) HAADF-STEM images of Rh/CC3-R-*homo* catalyst. (d) Size histograms of Rh NPs based on 300 NPs.

no signs of aggregation (Figure S3). It should be noted that the redispersion of MNPs after drying to solution has been often difficult because of the weak binding interaction between the supports and MNPs, easily leading to NP aggregation in solution.¹¹ Presumably, the CC3-R here provides good solubility as well as effectively anchors the Rh NPs' surface, thus preventing them from aggregation.

It is well-known that ammonia borane (NH₃BH₃, AB) is a promising material for chemical hydrogen storage, from which hydrogen can be released through hydrolysis or methanolysis.^{12,13} In this work, methanolysis of AB is employed as a reaction for evaluating the catalytic activity of Rh/CC3-R-*homo* catalyst. The reaction is initiated by introducing AB into the reaction flask containing the as-synthesized Rh/CC3-R-*homo* catalyst with vigorous shaking at room temperature (298 K). H₂ generated from the methanolysis of AB is collected in the buret, with which the H₂ volume is monitored. Figure 2 shows the H₂

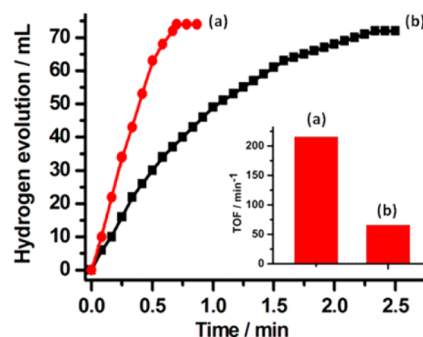


Figure 2. Time course plots of H₂ generation for the methanolysis of AB over the (a) Rh/CC3-R-*homo* and (b) Rh/CC3-R-*hetero* catalysts at 298 K (Rh/AB = 0.0199). Inset: the corresponding TOF values of the catalysts.

generation from AB in the presence of Rh/CC3-R-*homo* catalyst. The hydrogen release rate is highly dependent on the content of Rh (Figure S7). Under our evaluation conditions, the Rh/CC3-R-*homo* catalyst with Rh loading of 2.4 wt % shows the highest catalytic activity, with which the reaction can be completed (H₂/AB = 3.0) within 0.7 min (Rh/AB = 0.0199) at 298 K (Figure 2a), giving a TOF value as high as 215.3 mol of H₂ per mol of Rh per

min, which, notably, is the highest value among the catalysts ever reported for methanolysis of AB reaction.¹³ Such extremely excellent catalytic performance demonstrates that the present homogenized heterogeneous catalyst is effective for liquid-phase catalytic reaction.

It is reasonable that such unexpected high catalytic activity is attributed to the ultrasmall Rh NPs with highly accessible catalytic sites in solution, which is favorable for the direct contact between the reactants and Rh NPs. To further demonstrate our hypothesis, the corresponding heterogeneous catalyst Rh/CC3-*R-hetero* in a form of solid toward AB methanolysis is compared. The powder sample of Rh/CC3-*R-hetero* is obtained by direct drying freshly prepared Rh/CC3-*R-homo* catalyst in N₂ flow atmosphere, and then the resultant solid is mixed with methanol solution for the use of AB methanolysis reaction. It is notable that the Rh/CC3-*R-hetero* catalyst is insoluble in methanol, which provides the heterogeneous condition for AB methanolysis reaction. As shown in Figure 2b, the catalytic reaction by the Rh/CC3-*R-hetero* catalyst is completed (H₂/AB = 3.0) within 2.3 min (Rh/AB = 0.0199) at room temperature (298 K), giving a TOF value of 65.5 mol of H₂ per mol of Rh per min (Figure 2b). Such a kinetic rate is much lower than that of Rh/CC3-*R-homo* catalyst. It is notable that the catalyst obtained by redissolving the Rh/CC3-*R-hetero* in pure dichloromethane solution is inactive toward H₂ release reaction (Figure S8). These experiments unequivocally demonstrate the role of soluble cage in promoting the kinetics of liquid-phase catalytic reaction. To further demonstrate the importance of the CC3-*R* stabilizer/homogenizer in liquid-phase catalysis, the control experiment by using support-free catalyst (Rh-SP-Free) for AB methanolysis under the condition similar to that of Rh/CC3-*R-homo* catalyst is performed. Figure S9 shows that the completion of reaction needs as long as 35 min (Rh/AB = 0.0199), with a TOF of 4.3 mol of H₂ per mol of Rh per min, which is only 1/50 of Rh/CC3-*R-homo* catalyst. Actually, the obtained Rh-SP-Free catalyst shows serious aggregations through reduction of metal precursor by NaBH₄ without CC3-*R* (Figure S10). We have also performed the catalytic reaction based on the conventional surfactant polyvinylpyrrolidone (PVP) protected Rh NP catalyst (Rh-PVP), which also gives a poor catalytic kinetic with a TOF of 15.1 mol of H₂ per mol of Rh per min (Figure S11). These control experiments indicate that the soluble cage can successfully serve as not only stabilizers but also efficient dispersing agents for the synthesis of MNPs in solution. Moreover, the catalytic activity of soluble catalyst is much higher than its heterogeneous counterpart toward the same liquid-phase catalytic reaction, which highlights the advantage of using such strategy in improving the catalytic performance. This is understandable because the cage features intrinsic characteristics of high solubility and dispersibility in certain solvents, which make them act as stabilizing/homogenizing agents for the MNPs to prevent them from aggregation. In addition, the functional group (C=N) can efficiently anchor MNPs and thus control their size and distribution on the cage during the synthetic process. Moreover, the absence of long alkyl chains on the cages provides the MNPs with more available active sites. Especially, the open skeleton of cage provides much higher accessibility than the conventional surfactant for reactants to the active sites. Such characteristics in principle could boost the kinetics of the catalytic process.

The present strategy can be extended to other liquid-phase catalytic reactions with enhanced catalytic performance. Here, the catalytic performance of catalyst is investigated by employing the catalytic reaction reduction of 4-nitrophenol (4-NPh) in the

solution by NaBH₄ to produce 4-aminophenol (4-AMPh) as another model reaction. The conversion of 4-NPh can be readily monitored by UV-vis spectra, recording the change of characteristic absorbance at $\lambda = 400$ nm in alkaline solution. As shown in Figure 3a, the Rh/CC3-*R-homo* catalyst gives complete

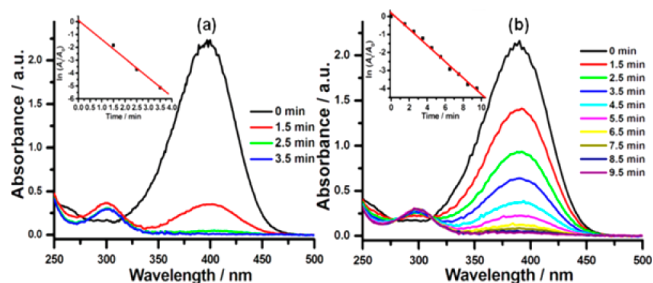


Figure 3. UV-vis spectra showing gradual reduction of 4-NPh over (a) Rh/CC3-*R-homo* and (b) Rh/CC3-*R-hetero* catalysts at room temperature. Inset: the corresponding slope of the plot $\ln(A_t/A_0)$ vs time (min).

conversion in 3.5 min (Rh/4-NPh/NaBH₄ (mol/mol/mol) = 1/21/16596). A linear correlation of $\ln(A_t/A_0)$ versus time (A_t and A_0 represent the absorbance at the intervals and the initial stage of 4-nitrophenolate ion, respectively) is obtained (Figure 3a inset), and the pseudo-first-order rate constant (k) is estimated to be $2.5 \times 10^{-2} \text{ s}^{-1}$. Such catalytic activity is superior to that of Rh-based catalysts under ambient conditions.¹⁴ In contrast, the corresponding heterogeneous catalyst Rh/CC3-*R-hetero* gives a lower catalytic activity under similar condition as inferred from Figure 3b. The estimated rate constant k value is $0.75 \times 10^{-2} \text{ s}^{-1}$. Such enhanced catalytic activity further demonstrates that the present strategy could be generalized to other liquid-phase reactions with enhanced the catalytic activities.

Durability and recyclability of MNPs are important parameters for potential applications of the catalysts. Typically, MNP-based catalysts suffer from both low separation efficiency from reaction system, owing to their overall small size, and reduced catalytic activity caused by coagulation of MNPs during reactions. The present Rh/CC3-*R-homo* catalyst can overcome these challenges. We have chosen AB methanolysis reaction to check the durability and recyclability of Rh/CC3-*R-homo* catalyst. The durability of Rh/CC3-*R-homo* catalyst is examined by successively adding AB into the reactor after completion of the previous run, and no significant loss in activity and selectivity is observed over 5 cycles (Figure S15). After catalytic experiments, we analyze Rh/CC3-*R-homo* catalyst by STEM-HAADF measurements, which clearly reveal that the size and morphology of Rh NPs remain the same even after catalytic reaction (Figure S16). In fact, after completion of the reaction, the catalyst could be recovered by drying in a N₂ flow atmosphere and washing with water and methanol (Figure S3). The PXRD measurement reveals that the crystalline characteristic of CC3-*R* is preserved, and no noticeable peaks from Rh NPs are detected, indicating the high stability of catalysts after catalytic reaction (Figure S1). Moreover, the dried sample can redissolve in the dichloromethane-methanol mixture without precipitation (Figure S3), which can be further used for catalytic reaction (Figure S17). Therefore, the present Rh/CC3-*R-homo* catalyst possesses the advantages of both homogeneous and heterogeneous catalysts with high dispersibility and stability and excellent recyclability, which are essential for its superior catalytic performance.

In conclusion, for the first time, a facile method to homogenize heterogeneous Rh NP catalyst has been developed based on the immobilization to soluble porous organic cage CC3-R. The soluble cage molecule with an intrinsic open channel provides unique properties as a versatile platform to immobilize MNPs and exhibits an unexpected talent for controlling of MNPs in an ultrasmall size, preventing them from aggregation and providing high stability and dispersibility in solution. Illustrating the application of this method, Rh/CC3-R-homo catalyst shows superior catalytic performances toward the AB methanolysis and 4-NPh reduction reactions. The activities are much higher than those of the heterogeneous counterpart. Moreover, the Rh/CC3-R-homo catalyst exhibits excellent durability and reusability. Considering the facile process of catalyst preparation, the present strategy could be easily expanded to prepare other kinds of MNPs for various liquid-phase catalytic applications by using a soluble cage stabilizer/homogenizer. Moreover, the present work may bring new inspiration to the catalysis field in terms of the exploration of advanced catalysts that combine the merits of both homo- and heterogeneous catalysts.

■ ASSOCIATED CONTENT

● Supporting Information

Experimental details, sorption isotherms, PXRD patterns, XPS, UV-vis spectra, catalytic reaction data, and TEM images for Rh NPs. The Supporting Information is available free of charge on the ACS Publications website at DOI: 10.1021/jacs.5b04029.

■ AUTHOR INFORMATION

Corresponding Author

*q.xu@aist.go.jp

Notes

The authors declare no competing financial interest.

■ ACKNOWLEDGMENTS

The authors thank AIST for financial support. J.K.S. thanks JSPS for a postdoctoral fellowship.

■ REFERENCES

- (1) (a) McKeown, N. B.; Budd, P. M. *Chem. Soc. Rev.* **2006**, *35*, 675. (b) Meilikhov, M.; Yusenko, K.; Esken, D.; Turner, S.; Van Tendeloo, G.; Fischer, R. A. *Eur. J. Inorg. Chem.* **2010**, 3701. (c) Kaur, P.; Hupp, J. T.; Nguyen, S. T. *ACS Catalysis* **2011**, *1*, 819. (d) Dhakshinamoorthy, A.; Garcia, H. *Chem. Soc. Rev.* **2012**, *41*, 5262. (e) Moon, H. R.; Lim, D. W.; Suh, M. P. *Chem. Soc. Rev.* **2013**, *42*, 1807. (f) Aijaz, A.; Xu, Q. *J. Phys. Chem. Lett.* **2014**, *5*, 1400. (g) Zhao, M.; Ou, S.; Wu, C. D. *Acc. Chem. Res.* **2014**, *47*, 1199.
- (2) (a) Ma, L.; Abney, C.; Lin, W. *Chem. Soc. Rev.* **2009**, *38*, 1248. (b) Chan-Thaw, C. E.; Villa, A.; Katekomol, P.; Su, D.; Thomas, A.; Prati, L. *Nano Lett.* **2010**, *10*, 537. (c) Ding, S. Y.; Gao, J.; Wang, Q.; Zhang, Y.; Song, W. G.; Su, C. Y.; Wang, W. *J. Am. Chem. Soc.* **2011**, *133*, 19816. (d) Xu, H.; Chen, X.; Gao, J.; Lin, J.; Addicoat, M.; Irle, S.; Jiang, D. *Chem. Commun.* **2014**, 50, 1292. (e) Li, L.; Matsuda, R.; Tanaka, I.; Sato, H.; Kanoo, P.; Jeon, H. J.; Foo, M. L.; Wakamiya, A.; Murata, Y.; Kitagawa, S. *J. Am. Chem. Soc.* **2014**, *136*, 7543. (f) Gu, Z. Y.; Park, J.; Raiff, A.; Wei, Z.; Zhou, H. C. *ChemCatChem* **2014**, *6*, 67. (g) Nasalevich, M. A.; Becker, R.; Ramos-Fernandez, E. V.; Castellanos, S.; Veber, S. L.; Fedin, M. V.; Kapteijn, F.; Reek, J. N. H.; van der Vlugt, J. I.; Gascon, J. *Energy Environ. Sci.* **2015**, *8*, 364.
- (3) (a) Hasell, T.; Wood, C. D.; Clowes, R.; Jones, J. T. A.; Khimyak, Y. Z.; Adams, D. J.; Cooper, A. I. *Chem. Mater.* **2010**, *22*, 557. (b) Aijaz, A.; Karkamkar, A.; Choi, Y. J.; Tsumori, N.; Rönnebro, E.; Autrey, T.; Shioyama, H.; Xu, Q. *J. Am. Chem. Soc.* **2012**, *134*, 13926. (c) Na, K.; Choi, K. M.; Yaghi, O. M.; Somorjai, G. A. *Nano Lett.* **2014**, *14*, 5979.
- (4) (a) Copéret, C.; Chabanas, M.; Saint-Arroman, R. P.; Basset, J. M. *Angew. Chem., Int. Ed.* **2003**, *42*, 156. (b) Buchwalter, P.; Rosé, J.; Braunstein, P. *Chem. Rev.* **2015**, *115*, 28.
- (5) (a) Zhao, X. S.; Bao, X. Y.; Guo, W.; Lee, F. Y. *Mater. Today* **2006**, *9*, 32. (b) White, R. J.; Luque, R.; Budarin, V. L.; Clark, J. H.; Macquarrie, D. J. *Chem. Soc. Rev.* **2009**, *38*, 481. (c) Goel, S.; Wu, Z.; Zones, S. I.; Iglesia, E. *J. Am. Chem. Soc.* **2012**, *134*, 17688.
- (6) Niu, Z. Q.; Li, Y. D. *Chem. Mater.* **2014**, *26*, 72.
- (7) (a) Cole-Hamilton, D. J. *Science* **2003**, 1702. (b) Astruc, D.; Lu, F.; Aranzas, J. R. *Angew. Chem., Int. Ed.* **2005**, *44*, 7852. (c) de Almeida, M. P.; Carabineiro, S. A. C. *ChemCatChem* **2012**, *4*, 18.
- (8) (a) Shi, F.; Tse, M. K.; Pohl, M. M.; Brückner, A.; Zhang, S.; Beller, M. *Angew. Chem., Int. Ed.* **2007**, *46*, 8866. (b) Witham, C. A.; Huang, W.; Tsung, C.; Kuhn, J. N.; Somorjai, G. A.; Toste, F. D. *Nat. Chem.* **2010**, *2*, 36. (c) Gross, E.; Liu, J. H. C.; Toste, F. D.; Somorjai, G. A. *Nat. Chem.* **2012**, *4*, 947. (d) Genna, D. T.; Wong-Foy, A. G.; Matzger, A. J.; Sanford, M. S. *J. Am. Chem. Soc.* **2013**, *135*, 10586. (e) Moret, S.; Dyson, P. J.; Laurenczy, G. *Nat. Commun.* **2014**, *5*, 4017.
- (9) (a) Tozawa, T.; Jones, J. T. A.; Swamy, S. I.; Jiang, S.; Adams, D. J.; Shakespeare, S.; Clowes, R.; Bradshaw, D.; Hasell, T.; Chong, S. Y.; Tang, C.; Thompson, S.; Parker, J.; Trewin, A.; Bacsa, J.; Slawin, A. M. Z.; Steiner, A.; Cooper, A. I. *Nat. Mater.* **2009**, *8*, 973. (b) Hasell, T.; Chong, S. Y.; Jelfs, K. E.; Adams, D. J.; Cooper, A. I. *J. Am. Chem. Soc.* **2012**, *134*, 588.
- (10) Mévellec, V.; Leger, B.; Mauduit, M.; Roucoux, A. *Chem. Commun.* **2005**, 2838.
- (11) (a) Leifert, A.; Pan-Bartnek, Y.; Simon, U.; Jahnen-Dechent, W. *Nanoscale* **2013**, *5*, 6224. (b) Strayer, M. E.; Binz, J. M.; Tanase, M.; Shahri, S. M. K.; Sharma, R.; Rioux, R. M.; Mallouk, T. E. *J. Am. Chem. Soc.* **2014**, *136*, 5687.
- (12) (a) Gutowska, A.; Li, L.; Shin, Y.; Wang, C. M.; Li, X. S.; Linehan, J. C.; Smith, R. S.; Kay, B. D.; Schmid, B.; Shaw, W.; Gutowski, M.; Autrey, T. *Angew. Chem., Int. Ed.* **2005**, *44*, 3578. (b) Keaton, R. J.; Blacquiere, J. M.; Baker, R. T. *J. Am. Chem. Soc.* **2007**, *129*, 1844. (c) Kim, S. K.; Han, W. S.; Kim, T. J.; Kim, T. Y.; Nam, S. W.; Mitoraj, M.; Piekos, L.; Michalak, A.; Hwang, S. J.; Kang, S. O. *J. Am. Chem. Soc.* **2010**, *132*, 9954. (d) Zhu, Q. L.; Xu, Q. *Energy Environ. Sci.* **2015**, *15*, 478.
- (13) (a) Ramachandran, P. V.; Gagare, P. D. *Inorg. Chem.* **2007**, *46*, 7810. (b) Kalidindi, S. D.; Vernekar, A. S.; Jadigar, B. R. *Phys. Chem. Chem. Phys.* **2009**, *11*, 770. (c) Caliskan, S.; Zahmakıran, M.; Özkır, S. *Appl. Catal., B* **2010**, *93*, 387. (d) Yadav, M.; Xu, Q. *Energy Environ. Sci.* **2012**, *5*, 9698.
- (14) (a) Kundu, S.; Wang, K.; Liang, H. *J. Phys. Chem. C* **2009**, *113*, 18570. (b) Moitra, N.; Kanamori, K.; Ikuhara, Y. H.; Gao, X.; Zhu, Y.; Hasegawa, G.; Takeda, K.; Shimada, T.; Nakanishi, K. *J. Mater. Chem. A* **2014**, *2*, 12535.